10-1-2007

A Statistical Model to Forecast Short-Term Atlantic Hurricane Intensity

Kevin Law
Marshall University, law14@marshall.edu

Jay S. Hobgood

A Statistical Model to Forecast Short-Term Atlantic Hurricane Intensity

KEVIN T. LAW

Department of Geography, Marshall University, Huntington, West Virginia

JAY S. HOBGOOD

Department of Geography, The Ohio State University, Columbus, Ohio

(Manuscript received 11 October 2005, in final form 15 December 2006)

ABSTRACT

An alternative 24-h statistical hurricane intensity model is presented and verified for 13 hurricanes during the 2004–05 seasons. The model uses a new method involving a discriminant function analysis (DFA) to select from a collection of multiple regression equations. These equations were developed to predict the future 24-h wind speed increase and the 24-h pressure drop that were constructed from a dataset of 103 hurricanes from 1988 to 2003 that utilized 25 predictors of rapid intensification. The accuracy of the 24-h wind speed increase models was tested and compared with the official National Hurricane Center (NHC) 24-h intensity forecasts, which are currently more accurate on average than other 24-h intensity models. Individual performances are shown for Hurricanes Charley (2004) and Katrina (2005) along with a summary of all 13 hurricanes in the study. The average error for the 24-h wind speed increase models was 11.83 kt (1 kt = 0.5144 m s^{-1}) for the DFA-selected models and 12.53 kt for the official NHC forecast. When the DFA used the correctly selected model (CSM) for the same cases, the average error was 8.47 kt. For the 24-h pressure reduction models, the average error was 7.33 hPa for the DFA-selected models, and 5.85 hPa for the CSM. This shows that the DFA performed well against the NHC, but improvements can still be made to make the accuracy even better.

1. Introduction

Significant improvements have been made in operational forecasts of the movement of tropical cyclones over recent years (McAdie and Lawrence 2000), but the skill of intensity forecasts still lags that of track forecasts (DeMaria and Kaplan 1999; DeMaria et al. 2005). The improvements in track forecast skill at 3 days helped facilitate extending forecasts out to 5 days (Knaff et al. 2003). However, when a hurricane rapidly intensifies, the skill of the intensity forecasts decreases substantially. For example, in the Atlantic, Hurricanes Opal (1995) and Bret (1999) rapidly intensified to category 4 on the Saffir–Simpson scale (Saffir 1973; Simpson 1974) within 48 h of making landfall in the United States (Lawrence et al. 2001; Kaplan and DeMaria 2003) and then weakened to a category 3 hurricane just before landfall. More recently, Hurricane Charley (2004) rapidly intensified to a category 4 hurricane prior to making landfall near Cayo Costa, Florida. The central pressure in Charley dropped 18 hPa and the maximum sustained winds increased 30 kt (1 kt = 0.5144 m s^{-1}) in a 6-h period. The official 24-h forecast from the National Hurricane Center (NHC) (1800 UTC 12 August), when Charley was a category 2 hurricane with winds of 90 kt and a pressure of 980 hPa, called for an increase of 15 kt in the maximum sustained wind speed. The NHC forecast predicted that Charley would become a category 3 hurricane with winds of 105 kt. However, the maximum sustained wind speed actually increased 35 kt to 125 kt making it a strong category 4 hurricane. Improvements in intensity forecasts still need to be made, particularly when the hurricane starts to intensify rapidly.

The lower skill of the intensity forecasts is caused by the partial understanding of rapid intensification (Kaplan and DeMaria 2003). The role of the ocean, inner-core processes, and environmental changes have been investigated, but the majority of the studies have inves-

Corresponding author address: Dr. Kevin T. Law, Dept. of Geography, Marshall University, 211 Harris Hall, 1 John Marshall Dr., Huntington, WV 25755.
E-mail: law14@marshall.edu

DOI: 10.1175/WAF1027.1

tigated these topics individually. Comprehensive studies of the combined impacts of these factors on rapid intensification are limited. As a result, the precise physical mechanisms that cause rapid intensification are not well understood. The earliest studies tended to focus on the role and the benefits of warm ocean water upon intensity (e.g., Byers 1944; Miller 1958; Malkus and Riehl 1960). Warm core eddies have been a recent topic of interest and helped explain why Hurricane Opal rapidly intensified in the Gulf of Mexico (Shay et al. 2000). Willoughby et al. (1982) investigated the inner-core processes through the concept of eyewall replacement cycles that could produce intensity changes. Other studies have investigated environmental effects, most notably vertical wind shear, which have been shown to have significant impacts on hurricane development (Gray 1968; Merrill 1988). DeMaria and Kaplan (1994) developed the Statistical Hurricane Intensity Prediction Scheme (SHIPS), which featured vertical wind shear, in addition to oceanic parameters, as a significant predictor in the intensity model.

Several models are used today to forecast hurricane intensity including SHIPS; Statistical Hurricane Forecast (SHIFOR5), which is a 5-day forecast model; and the Geophysical Fluid Dynamics Laboratory (GFDL) model. The SHIFOR5 forecast errors in 2004 were approximately 10%–20% higher than the previous 10-yr mean, which suggested that the 2004 hurricanes were more difficult to forecast (Franklin 2005). According to Franklin, SHIFOR5 had a mean error of 13.6 kt at the 24-h forecast period. The official NHC forecast had a mean error of 10.2 kt at the same forecast period. In fact, the official NHC forecast had a lower mean error than all of the intensity models at the 24-h forecast period. Only two variants of the GFDL model were consistently skillful at the 24-h forecast period, whereas the statistical models tended to outperform the dynamic models especially at the short-term forecast intervals. The purpose of this paper is to present an alternative method to a statistical 24-h intensity model. The premise of this study is that different statistical models must be applied for different intensities of hurricanes and at different stages during the life cycle of the hurricane. Rather than using one regression model for a particular forecast interval, the model presented here uses a discriminant function analysis that selects from a collection of 24-h regression models, which is used to predict both the future 24-h wind speed increase and the future 24-h pressure decrease.

The data and analysis are presented in section 2, while the methods are presented in section 3. Results from the DFA statistical procedure are discussed in section 4 in addition to the case studies of Hurricanes Charley and Katrina. These hurricanes were chosen because they provide a good comparison in which the DFA performed well and poorly. A summary of the average errors for the 13 hurricanes in the study is also shown in section 4. The results for the 24-h wind speed increase model are compared with the official NHC forecasts particularly at the time of the rapid intensification for the hurricane. Finally, section 5 is the conclusion of the paper.

2. Data and analysis

This study examined all Atlantic basin hurricanes from 1988 to 2003 for a total of 103 hurricanes. Because this study was concerned with the factors that cause a hurricane to rapidly intensify, the entire track of each hurricane was not analyzed. Only the rapid intensification period (RIP) and the 60-h period prior to the RIP were analyzed for each hurricane. A RIP is defined as the 24-h period that experienced the most rapid decrease of central pressure. Therefore the pressure drop in each hurricane's RIP varied across the sample. Figure 1 shows the frequency distribution of the pressure drop of the RIPs in the sample. The distribution is skewed because of some extreme rapid hurricane intensification, including Hurricane Gilbert (1988), in which the pressure dropped 72 hPa in 24 h. Table 1 shows the list of variables that were examined in the sample. Each variable was evaluated at 6-h intervals starting at 60 h before the RIP and ending at the conclusion of the RIP. The study consisted of 16 data points for all 103 hurricanes, which contributed 1648 cases across the sample.

The latitude, longitude, central pressure, translational speed, inception time, wind speed, and previous 6-h wind speed change were obtained from the NHC hurricane database (HURDAT) file (Jarvinen et al. 1984). Inception time is defined as the number of hours after the initial advisory is given by the NHC. The data are available at 6-hourly intervals for all named Atlantic tropical cyclones from 1851 to the present. The vertical wind shear, relative humidity, mean sea level pressure (MSLP), and sea surface temperature (SST) data were obtained from the National Centers for Environmental Prediction–National Center for Atmospheric Research reanalysis dataset (Kalnay et al. 1996). The 6-hourly reanalysis data exist on a $2.5^\circ \times 2.5^\circ$ latitude–longitude grid, which translates into an approximate 210-km horizontal resolution. Data are available for 17 pressure levels but only the lowest significant levels from 925 to 70 hPa were needed to calculate the maximum potential intensity (MPI). The 925-, 850-, 700-, and 500-hPa levels were used to calculate the low- to

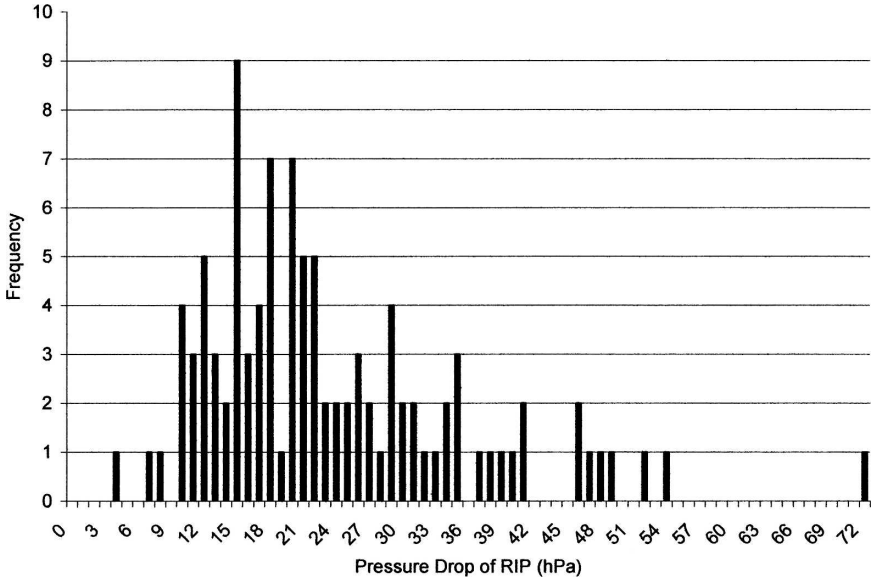

FIG. 1. The 24-h pressure drop during the RIP of the 103-hurricane sample.

midlevel relative humidity and the 850-, 500-, 200-, and 100-hPa levels were used to calculate the vertical wind shear in multiple layers. The storm center obtained from the HURDAT file was repositioned to the closest grid point and assumed to be the center of the hurricane for the purpose of this study. To smooth any extremes in the variables and to capture the magnitude over the entire storm, data from the analyses were averaged over a 5×5 grid of points centered around the storm center (Fig. 2). The data from the 25 grid points, in essence a $10^\circ \times 10^\circ$ latitude–longitude grid, were averaged together to obtain a magnitude for the variable. Other size grids were tested (e.g., 3×3 and 7×7), but this size provided the best smoothed values.

TABLE 1. List of 25 variables.

Variable	Units	Definition
Lat	°N	Latitude
Long	°W	Longitude
850–500shr	m s^{-1}	850–500-hPa vertical shear
850–500dir	°	850–500-hPa vertical shear direction
850–200shr	m s^{-1}	850–200-hPa vertical shear
850–200dir	°	850–200-hPa vertical shear direction
850–100shr	m s^{-1}	850–100-hPa vertical shear
850–100dir	°	850–100-hPa vertical shear direction
500–200shr	m s^{-1}	500–200-hPa vertical shear
500–200dir	°	500–200-hPa vertical shear direction
925RH	%	925-hPa relative humidity
850RH	%	850-hPa relative humidity
700RH	%	700-hPa relative humidity
500RH	%	500-hPa relative humidity
MSLP	hPa	Mean sea level pressure
SST	K	Sea surface temperature
MPI	hPa	Maximum potential intensity
CentPres	hPa	Central pressure
AttMPI	%	Attained MPI
TransSp	m s^{-1}	Translational speed
HeatPot	kJ cm^{-2}	Hurricane heat potential
CoreHP	kJ cm^{-2}	Core hurricane heat potential
Incep	h	Inception time
Prev6	kt	Previous 6-h wind speed change
WindSp	kt	Wind speed

SST data were available on a weekly time scale at a $1^\circ \times 1^\circ$ latitude–longitude resolution; however, the grid boxes were adjusted to match the sizes of the other variables. The SSTs were derived from in situ (ship and buoy) data, satellites, and simulated sea surface temperatures for areas covered by sea ice. Before these datasets are calculated, they are adjusted for biases using the simulated SSTs as the external boundary condition, which is described by Reynolds (1988) and Reynolds and Marsico (1993). An explanation of the ocean interaction analysis can also be found in Reynolds and Smith (1994).

The Holland method was used to compute MPI in this study. Because tropical cyclones derive their energy from latent heat release in the environment, the MPI is estimated as a function of the available thermodynamic energy in the environment and usually expressed in terms of pressure. Therefore, the MPI is simply the lowest theoretical pressure a tropical cyclone can achieve under ideal conditions. The Holland method (Holland 1997) is a purely thermodynamic approach of predicting the MPI of tropical cyclones.

The Holland method consists of three parts. First, the moist-adiabatic lapse rate is calculated. Next, an itera-

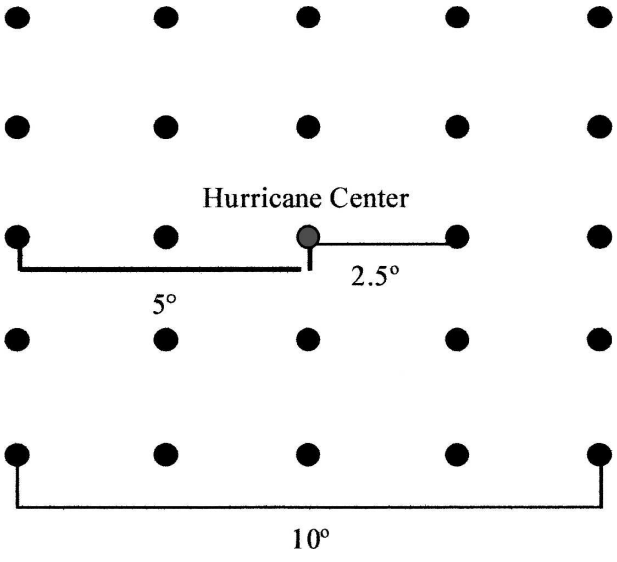

FIG. 2. The 5 × 5 grid "box" averaging technique.

tive process is used to estimate the equivalent potential temperature. The surface equivalent potential temperature is calculated from the environmental temperature and pressure, in addition to the sea surface temperature and eyewall relative humidity. Once the equivalent potential temperature is calculated, the pressure of the column drops hydrostatically due to subsidence warming. A new surface pressure causes a new equivalent potential temperature to be recalculated. The process continues until the surface pressure changes less than 1 hPa. When the surface pressure calculations converge, the eye temperature profile and the hydrostatic decrease of central pressure due to the formation of the eye are calculated if the eyewall deficit is more than 20 hPa from the environment. From these calculations, the MPI is estimated:

$$\mathrm{MPI} = P_{\mathrm{Senv}} - \Delta P_{\mathrm{Smax}}, \tag{1}$$

where P_{Senv} is the surface pressure of the environment and ΔP_{Smax} is the maximum achievable surface pressure fall. The hydrostatic change in surface pressure can be found by the following:

$$\Delta P_S = \frac{P_S}{T_v(P_S)} \int_{P_S}^{P_T} \Delta T_v \, d \ln p, \tag{2}$$

where P_S is the surface pressure and T_v is the virtual temperature.

Usually, lower central pressures indicate more intense tropical cyclones. Therefore, if a hurricane has a low MPI, it has a greater potential to become a powerful hurricane assuming there are no detrimental factors affecting it.

However, MPI by itself is not a good indicator of the intensity of a tropical cyclone because it is a measure of how intense the storm could potentially become. The attained MPI, which incorporates the MPI with the central pressure and ambient MSLP, indicates as a percentage how close a hurricane is to its MPI and is given as

$$\left(1 - \frac{\mathrm{MPI} - \mathrm{CentPres}}{\mathrm{MPI} - \mathrm{MSLP}}\right) \times 100\%. \tag{3}$$

The attained MPI is a better indicator of how strong a hurricane is because it considers the actual central pressure (Law 2001).

The hurricane heat potential and core hurricane heat potential annual climatology data were obtained from the Atlantic Oceanographic and Meteorological Laboratory (AOML) and are available weekly on a 1° latitude–longitude grid beginning in 1992. Seasonal climatology data are now available through the Joint Hurricane Test Bed program (Mainelli 2000; DeMaria et al. 2005) and would provide a more refined input option for future models. The tropical cyclone heat potential (or sometimes referred to as hurricane heat potential) is defined as the integrated vertical temperature from the sea surface to the depth of the 26°C isotherm. This is calculated using four points from altimeter-derived vertical temperature profile estimates in the upper ocean. Those four points include the sea surface temperature obtained from the Tropical Rainfall Measuring Mission's Microwave Imager fields (Reynolds et al. 2004; Wentz and Meissner 1999), the altimeter estimates of the 20°C isotherm within a two-layer reduced-gravity scheme (Goni et al. 1997), and the depth of the 26°C isotherm from a climatological relationship between the depths of both the 20° and the 26°C isotherms.

A two-layer reduced-gravity ocean model is used to monitor the upper-layer thickness (Goni et al. 1997), which is defined as the depth from the sea surface to the 20°C isotherm. The 20°C isotherm is selected because it lies in the middle of the main thermocline, which is often seen as an indicator of the upper-layer flow especially found in the Gulf of Mexico and the western tropical Atlantic. Therefore, the 20°C isotherm separates two layers of differing densities. The upper-layer thickness (h_1) can be estimated from the altimeter-derived sea height anomaly (η') if the mean upper-level thickness ($\overline{h_1}$) and reduced-gravity (g') fields are known based upon the following equation:

$$h_1(x,y,t) = \overline{h_1}(x,y) + \frac{g}{g'(x,y)} \eta'(x,y,t), \tag{4}$$

where $g' = \varepsilon g$, g is the acceleration of gravity, and

$$\varepsilon(x,y) = \frac{\rho_2(x,y) - \rho_1(x,y)}{\rho_2(x,y)}, \quad (5)$$

where $\rho_1(x, y)$ and $\rho_2(x, y)$ represent the upper- and lower-level densities, respectively. Climatology based on Levitus (1984) is used to estimate g' and $\overline{h_1}$.

The tropical cyclone heat potential is then computed using the method defined by Leipper and Volgenau (1972) as the heat content of the upper layer relative to the depth on the 26°C isotherm:

$$Q(x,y,t) = 0.5\rho c_p \Delta T(x,y,t)\Delta z(x,y,t), \quad (6)$$

where ρ is the average oceanic density (1.026 g cm^{-3}), c_p is the specific heat at constant pressure (1 cal g^{-1} °C^{-1}), and ΔT is the difference between the SST and 26°C established over a depth Δz. The depth of the 26°C isotherm was found using a climatological relationship between the depths of the 20° and the 26°C isotherms. The core hurricane heat potential is similar to HeatPot except it is averaged over a 1° radius instead of a 5° radius.

3. Methods

The Law technique is highlighted by a two-step discriminant function analysis (DFA) procedure followed by a multiple regression analysis. DFA determines which predictors or variables best discriminate, better than chance, between two or more groups. Assuming the variables differ among the groups, the DFA will help classify each case into a particular group with which it closely corresponds. DFA was applied in order to help identify how strong the system would eventually become and how close it was to the RIP.

The first step of the DFA (Fig. 3) examined each case and determined if it had the characteristics of *becoming a major hurricane* or *at most, only becoming a minor hurricane*, which would also include tropical storms and depressions. After classifying each case into one of the two groups, the DFA then classified each case according to its proximity to the RIP. The "major hurricane" and "minor hurricane" cases from step one were separated and a second DFA was performed on each group based upon the four following categories:

- time segment 1—more than 48 h before the RIP,
- time segment 2—between 24 and 48 h before the RIP,
- time segment 3—less than 24 h before the RIP, and
- time segment 4—the RIP.

Therefore, after both steps of the DFA, each case is classified into one of eight possible groups (Fig. 3).

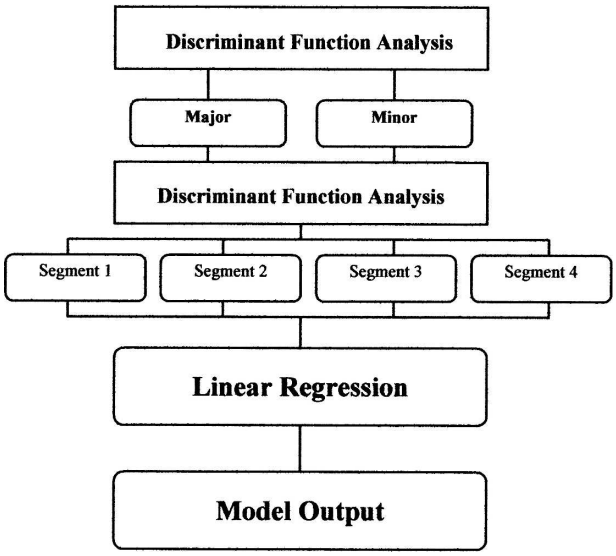

FIG. 3. Flowchart representation of the procedures used in the statistical analyses.

Eight multiple regression models were then created and applied to the appropriate cases.

A stepwise regression technique was applied to create the model for the eight different cases created by the DFA. In stepwise multiple regression, the predictor variable that has the highest correlation and is statistically significant at a particular threshold is entered into the regression. The next variable to be entered into the regression, assuming it is statistically significant, is the one that has the next highest correlation with the dependent variable while controlling for the variable that has already been entered. If the first variable still explains a significant amount of the variance while the second variable is controlled, then it is kept in the regression analysis. If not, the first variable is omitted from the analysis. This stepwise procedure is continued until there is no further significant increase in the explained variance by the independent variables.

Models for two different dependent variables were constructed using multiple regression analysis. The dependent variables were the following:

- future 24-h wind speed increase and
- future 24-h pressure drop.

The stepwise multiple regression was applied to all 1648 cases in the study. The cases were grouped into the eight possible combinations (Fig. 4), not by which the DFA selected, but by what actually occurred. Each variable used in the regression equation was significant at the 95% confidence interval. The regression equations that were created are shown in Tables 2 and 3. In

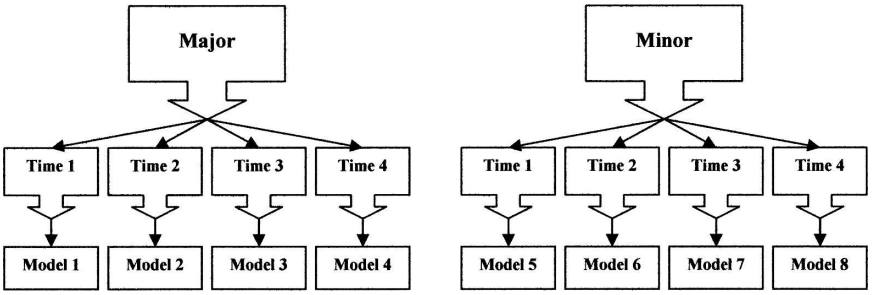

FIG. 4. Flowchart of eight possible models.

the 24-h pressure drop equations (Table 2) there was little repetition in the variables used in the eight models, which seems to suggest that different factors are responsible for intensification at different stages for both major and minor hurricanes. Variable repetition also was limited in the 24-h wind speed increase equations (Table 3). However, there was variable repetition between similar models for the 24-h pressure drop and wind speed increase. This seems to make sense because both the pressure fall and the wind speed increase are measures of how much the hurricane intensifies. For example, major hurricanes at time interval 1 (model 1) included MSLP, translational speed, and core heat potential as predictors for both 24-h pressure drop and wind speed increase. The core heat potential and the translational speed were the most significant for model 1 as major hurricanes typically have high heat potential at early stages. As the major hurricane progresses, SST and MPI are the most significant as these hurricanes have low MPIs and are over areas of high SSTs. Near the onset of the RIP, the wind speed and the core heat potential are usually high when model 3 is applied. During the RIP (model 4), MSLP, longitude, translational speed, and central pressure were used both as predictors for 24-h pressure drop and wind speed increase. Typically, the mean sea level pressures are low, the heat potential is high, and the translational speed is low enough for the hurricane to take advantage of the ocean energy.

As for the minor hurricane models, model 5 primarily uses the most significant variable, inception time, which often is very short because these storms have not developed for very long. Model 6 uses wind speed, MSLP, and SST, but these variables have negative coefficients, which explains why this minor hurricane model predicts less of a pressure drop than do the major hurricane models. Model 7 specifically looks at the previous 6-h change in wind speed and the 850-hPa relative humidity. The more humid the 850-hPa layer is and the more the wind speed increases, the greater the amount of pressure reduction is predicted. Finally, model 8 uses wind speed, longitude, and 850–100-hPa shear. The wind speed has a negative coefficient, meaning that strong minor hurricanes will usually not intensify much, preventing them from becoming major hurricanes.

The future 24-h wind speed models (Table 3) primarily use core heat potential and translational speed during early stages (model 1). This is consistent with the pressure models as high heat potential and higher translational speed predict stronger intensification. Model 2 uses attained MPI, 850–200-hPa shear, and translational speed. Major hurricanes typically have lower attained MPIs leading up to the RIP as this is a sign that a storm has more potential to intensify. The negative coefficient for the 850–200-hPa shear indicates that shear needs to be low for the hurricane to intensify, while the translational speed needs to continue to be

TABLE 2. Future 24-h pressure drop regression equations.

Model	Regression equation
Major, time segment 1 (model 1)	−0.692MSLP + 0.648TransSp + 0.096CoreHP + 702.316
Major, time segment 2 (model 2)	−0.783(850–500shr) + 0.08MPI + 4.785SST − 1502.349
Major, time segment 3 (model 3)	0.092CoreHP − 0.046Incep + 0.216WindSp + 0.245(500RH) − 0.591
Major, time segment 4 (model 4)	−1.012MSLP + 0.314HeatPot − 0.427Long − 3.148TransSp + 0.631CentPres + 460.375
Minor, time segment 1 (model 5)	−0.051(700RH) − 13.567AttMPI + 0.347Prev6 + 0.112Lat + 0.024Incep + 2.698
Minor, time segment 2 (model 6)	−0.08(850RH) − 0.722SST + 0.291TransSp − 0.117WindSp − 0.355MSLP + 0.017(850–100dir) + 587.07
Minor, time segment 3 (model 7)	−0.194(925RH) + 0.203(850RH) + 0.468Prev6 + 11.394
Minor, time segment 4 (model 8)	−0.390(850–100shr) − 0.024(850–500dir) − 0.182Long − 0.357WindSp + 44.081

TABLE 3. Future 24-h wind speed increase regression equations.

Model	Regression equation
Major, time segment 1 (model 1)	0.517TransSp + 0.260(925RH) + 0.138CoreHP + 0.575Prev6 − 14.351
Major, time segment 2 (model 2)	0.016(850–500dir) − 0.018(850–200dir) + 0.157(700RH) + 0.958TransSp − 0.642(850–200shr) − 40.290AttMPI + 13.012
Major, time segment 3 (model 3)	−0.199Long + 0.325(500RH) − 0.248MPI + 248.834
Major, time segment 4 (model 4)	0.394HeatPot − 4.067TransSp − 0.593Long − 0.700WindSp + 122.571
Minor, time segment 1 (model 5)	0.025Incep + 0.827Prev6 + 3.08
Minor, time segment 2 (model 6)	0.780(850–500shr) + 0.019(500–200dir) − 0.159(500RH) − 0.700MSLP − 0.395(850–200shr) − 0.390(850RH) − 0.794CentPres + 0.923TransSp − 0.796WindSp + 1570.089
Minor, time segment 3 (model 7)	0.02(850–500dir) + 0.665Prev6 − 0.524CentPres − 0.528WindSp + 560.58
Minor, time segment 4 (model 8)	0.098MPI + 0.323HeatPot − 0.467CentPres − 0.770(850–100shr) − 0.343Long − 1.095WindSp + 465.604

higher. Near the onset of the RIP, model 3 uses MPI (negative coefficient) as lower MPIs forecast a higher increase in wind speeds. During the RIP (model 4), the wind speed increase will start to taper off as indicated by the strong negative wind speed coefficient. Higher translational speeds also tend to be more detrimental during the RIP, as this can be a sign that the storm has been "captured" by the midlatitude westerlies and an extratropical transition has begun. During the early stages for minor hurricanes, model 5 uses previous 6-h wind speed and inception time. Model 6 primarily uses wind speed, central pressure, MSLP, and translational speed as seen with the pressure models, and model 7 also uses wind speed and central pressure. Often the wind speeds are lower and central pressures are lower for minor hurricanes leading up to the RIP, explaining why their coefficients are negative. Finally, model 8 included the 850–100-hPa shear, the 850–500-hPa shear direction, longitude, and the central pressure for both types of models. This further suggests that the intensification of hurricanes at similar stages in their life cycles tends to be affected by similar factors.

4. Results

a. Statistical results

In the sample dataset, which consisted of 103 hurricanes, there were a total of 1648 possible cases (103 hurricanes × 16 data points). Of the 1648 total cases, there were 432 cases that had at least one missing discriminant variable and were invalid. These cases were from the hurricanes in the sample from 1988 to early 1992 because the heat potential data were not yet available. Even though these were invalid cases for the discriminant analysis, they were still important and were used in the multiple regression analysis. Therefore, a total of 1216 valid cases were analyzed in the first step of the discriminant analysis.

Of the 1216 total cases, there were 528 cases that described major hurricanes and 688 cases that described minor hurricanes (Table 4). The discriminant analysis was able to correctly classify 450 of the 528 major hurricane cases for an accuracy rate of 85.2%. For the minor hurricanes, it was able to correctly classify 568 of the 688 minor hurricane cases for an accuracy rate of 82.6%. Overall, the discriminant analysis was able to correctly classify 1018 of the 1216 total valid cases or 83.7%, which is more accurate than would be achieved through random selection (50%). The key predictors that discriminated the most between major and minor hurricanes were inception time, central pressure, wind speed, 850–200-hPa wind shear, and heat potential as shown by the structure matrix in Table 5. The correlation between each variable and its relationship to becoming *at most a minor hurricane* is shown in the first column. For example, the negative correlation means that shorter inception times lead to a greater chance of only becoming a minor hurricane. These variables intuitively made sense because major hurricanes typically have longer inception times, lower central pressure, higher wind speeds, lower 850–200-hPa wind shear, and higher heat potential than minor hurricanes.

The second step of the discriminant analysis was able to correctly classify 65.1%, 43.8%, 50.6%, and 69.8% of the major hurricane cases for time segments 1, 2, 3, and 4, respectively (Table 6). Overall, out of the 570 total major hurricane cases, 330 cases were classified cor-

TABLE 4. Classification results of step 1 of the DFA.

		Predicted group membership		
	Major/minor	Major	Minor	Tot
Count	Major	450	78	528
	Minor	120	568	688
%	Major	85.2	14.8	100.0
	Minor	17.4	82.6	100.0

TABLE 5. Structure matrix for the DFA. The correlations that are in boldface are among the highest of the group.

	Correlation coef, step 1 of the DFA	Correlation coef, step 2 of the DFA (major)	Correlation coef, step 2 of the DFA (minor)
Lat	0.339	0.338	0.334
Long	0.056	0.172	0.084
850–500shr	0.249	−0.051	0.085
850–500dir	−0.178	−0.133	−0.074
850–200shr	**0.407**	0.082	0.115
850–200dir	−0.115	−0.207	−0.173
850–100shr	0.331	0.027	0.007
850–100dir	−0.179	−0.083	−0.138
500–200shr	0.326	0.113	0.112
500–200dir	−0.133	−0.129	−0.182
925RH	0.024	−0.028	0.017
850RH	−0.073	−0.059	−0.002
700RH	−0.170	−0.006	0.033
500RH	0.006	0.053	0.006
MSLP	0.237	−0.099	−0.177
SST	−0.224	−0.057	−0.301
MPI	0.233	0.024	0.283
CentPres	**0.491**	**−0.770**	**−0.612**
AttMPI	0.027	**0.743**	0.167
TransSp	−0.256	0.092	**0.600**
HeatPot	**−0.352**	−0.014	−0.190
CoreHP	−0.275	0.048	−0.116
Incep	**−0.503**	0.289	0.509
Prev6	−0.237	0.498	0.488
WindSp	**−0.483**	**0.825**	**0.791**

rectly for a 57.9% accuracy rate. The second step was also able to correctly classify 66.7%, 37.5%, 50.7%, and 77.9% of the minor hurricane cases for time segments 1, 2, 3, and 4, respectively, (Table 7) while correctly classifying 369 of the 646 total cases for an accuracy rate of 57.1%. The time selection accuracy rates for both types of hurricanes (57.9% for major and 57.1% for minor) were more accurate than would have predicted by random selection, which would have been 25% in this case.

The key predictors that were able to discriminate the time segment among major hurricanes were wind speed, central pressure, and attained MPI (Table 5). The wind speed gradually increases as the hurricane approaches its RIP, while the central pressure gradually decreases. Attained MPI values have been show to approximately reach 28% at the onset of the RIP for major hurricanes (Law 2001). As for minor hurricanes, the key time segment discriminating predictors were wind speed, central pressure, and translational speed (Table 5). The wind speed and central pressure vary similarly to major hurricanes except that the wind speeds are lower and the central pressures are higher. Most minor hurricanes have low translational speeds at early stages of their development, while some minor hurricanes can have high translational speeds at late stages in their development due to the storm being captured by the midlatitude westerlies and undergoing extratropical transition.

TABLE 6. Classification results for step 2 of the DFA for the major group.

		Predicted group membership				
	Time segment	1	2	3	4	Tot
Count	1	77	35	16	1	129
	2	45	60	38	7	150
	3	13	45	93	27	178
	4	6	10	47	146	209
%	1	59.7	27.1	12.4	0.8	100.0
	2	30.0	40.0	25.3	4.7	100.0
	3	7.3	25.3	52.2	15.2	100.0
	4	2.9	4.8	22.5	69.9	100.0

TABLE 7. Classification results for step 2 of the DFA for the minor group.

		Predicted group membership				
	Time segment	1	2	3	4	Tot
Count	1	139	30	32	10	211
	2	60	65	47	18	190
	3	23	30	78	31	162
	4	0	3	25	103	131
%	1	65.9	14.2	15.2	4.7	100.0
	2	31.6	34.2	24.7	9.5	100.0
	3	14.2	18.5	48.1	19.1	100.0
	4	0.0	2.3	19.1	78.6	100.0

The independent dataset was constructed to see how well the DFA-selected models performed during the 60 h prior to and through the RIP. The dataset consisted of 13 hurricanes from the 2004–05 seasons (Table 8). Two hurricanes, Charley (2004) and Katrina (2005), had contrasting DFA accuracies. These hurricanes are discussed along with a summary of the entire dataset.

b. Hurricane Charley

The track for Hurricane Charley is shown in Fig. 5 with the thin line depicting the 60 h prior to the RIP and the boldface line depicting the RIP. The DFA performed well by correctly classifying all 16 data points and by forecasting Charley to become a major hurricane up to 4 days before it actually attained major hurricane status. Charley exhibited some of the features, such as low wind shear while located over areas with high heat potential, that many other major hurricanes have. As for the time classification, the DFA was able to correctly classify 14 out of the 16 intervals correctly.

TABLE 8. Thirteen hurricanes in the independent dataset.

Alex (2004)	Ivan (2004)	Emily (2005)
Charley (2004)	Jeanne (2004)	Irene (2005)
Danielle (2004)	Karl (2004)	Katrina (2005)
Frances (2004)	Lisa (2004)	
Gaston (2004)	Dennis (2005)	

The two misclassifications occurred during time intervals 13 and 15 when it said to use model 3 instead of model 4. These intervals had lower shear and relatively higher central pressures, which were more characteristic of the time periods just prior to the RIP.

The 24-h wind speed increase model is shown in Table 9. The model forecasts were able to outperform the NHC forecasts on 9 of the first 12 intervals. During time interval 12 (the onset of the RIP), the model predicted the wind speed would increase 34.62 kt to approximately 125 kt or category 4 strength over the next 24 h. The impact of the heat potential was underestimated as the actual observed increase was 35 kt making it a category 4 at 125 kt, whereas the NHC said the winds would only increase 15 kt to 105 kt. Because landfall occurred within 24 h during time intervals 13–16, the model did overestimate the intensity. It is also interesting to look at the results, had the DFA selected the correct model to be used. The correctly selected model (CSM) is also shown in Table 9. For Hurricane Charley, time intervals 13 and 15 were misclassified as the DFA-selected model 3 to be used instead of model 4. The CSM did improve both misclassified intervals (time intervals 13 and 15) and the CSM did more accurately predict the intensity of time interval 13 than the NHC. Therefore, 10 of the 16 time intervals shown would have been more accurate than the NHC forecasts.

As for the 24-h pressure drop forecasts for Hurricane Charley (Table 9), the models predicted the pressure drop to be very close to the observations, most notably at time interval 12 (the onset of the RIP), where it predicted a future 24-h pressure drop of 32.19 hPa. At this point, the central pressure was 980 hPa and the observed 24-h drop was 43 hPa, giving Charley a central pressure of 947 hPa. Therefore, the model predicted that Charley would attain a pressure just under 958 hPa at time interval 12 when it was on the south side of Cuba and approximately a day from U.S. landfall. The CSM did offer improvement during time intervals 13 and 15 but the main reason the model struggled from time intervals 13 to 16 was because Charley would be making landfall within 24 h and the regression models do not take into account weakening due to movement over land.

c. Hurricane Katrina

Figure 6 shows the track for Hurricane Katrina with the thin line depicting the 60 h prior to the RIP and the boldface line depicting the RIP. Like Hurricane Charley, the DFA was able to correctly classify all 16 data points as becoming a major hurricane beginning with

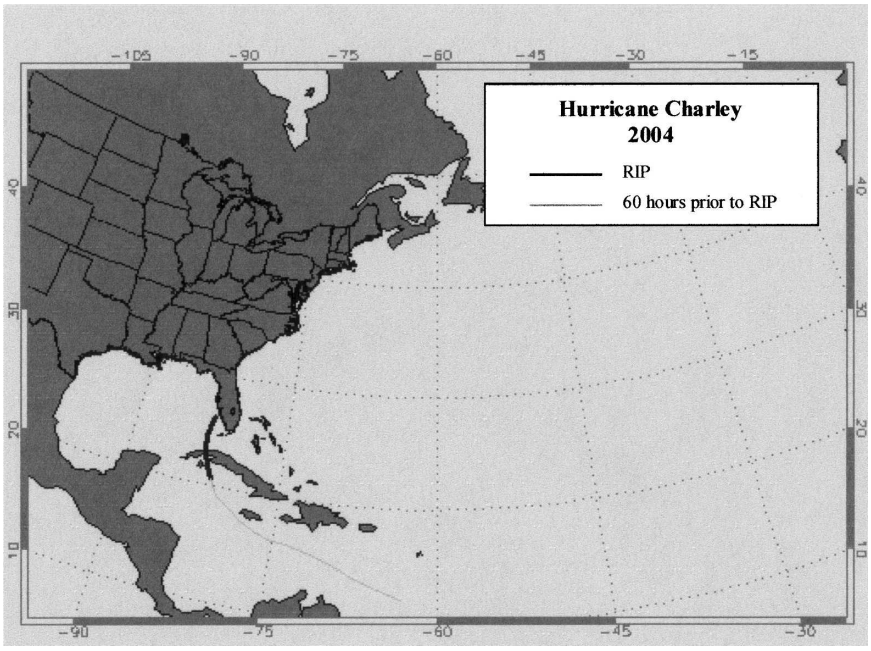

FIG. 5. Track of Hurricane Charley (2004).

TABLE 9. The model results for Hurricane Charley. The 24-h wind speed (WS) forecasts are shown with the observed values along with the 24-h pressure forecasts.

Time interval	Model	Model WS increase (kt)	Obs WS increase (kt)	NHC forecast (kt)	CSM (kt)	Model pressure drop (hPa)	Obs pressure drop (hPa)	CSM (hPa)
1	1	15.82	25	5	N/A	10.44	10	N/A
2	1	16.95	20	10	N/A	9.65	8	N/A
3	1	18.73	20	10	N/A	11.98	9	N/A
4	1	19.19	20	10	N/A	13.96	7	N/A
5	2	18.92	10	10	N/A	9.02	7	N/A
6	2	18.39	20	10	N/A	11.37	11	N/A
7	2	15.99	20	15	N/A	9.53	11	N/A
8	1	13.38	25	15	N/A	9.90	13	N/A
9	3	28.17	25	15	N/A	26.52	16	N/A
10	3	27.65	30	10	N/A	23.48	22	N/A
11	3	32.78	15	20	N/A	27.25	15	N/A
12	3	34.62	35	15	N/A	32.19	33	N/A
13*	3	35.35	−15	15	3.35	30.34	6	10.28
14	4	−12.40	−30	−15	N/A	−0.21	−27	N/A
15*	3	36.30	−30	−35	−9.68	30.50	−19	−1.47
16	4	−42.45	−65	−60	N/A	−26.74	−53	N/A

* Time intervals that were misclassified by the DFA.

time interval 1 when it was still a tropical storm and at least 18 h from achieving hurricane status. Katrina exhibited all of the classic characteristics of becoming a major hurricane, including very low 850–200-hPa vertical wind shear and the unusually high heat potential that was in the Gulf of Mexico. A warm core ring located in the central Gulf had extraordinary heat potential values over 100 kJ cm^{-2}. Passing over the warm core ring helped transform Katrina into a massive category 5 hurricane, which likely would not have occurred without the effect of the warm core ring. However, the DFA was not as accurate in selecting the time interval with respect to the RIP. It correctly classified only 5 of the 16 intervals because Katrina had such an unusually low pressure leading up to the RIP. The DFA classified it only 6 h away from the RIP when Katrina

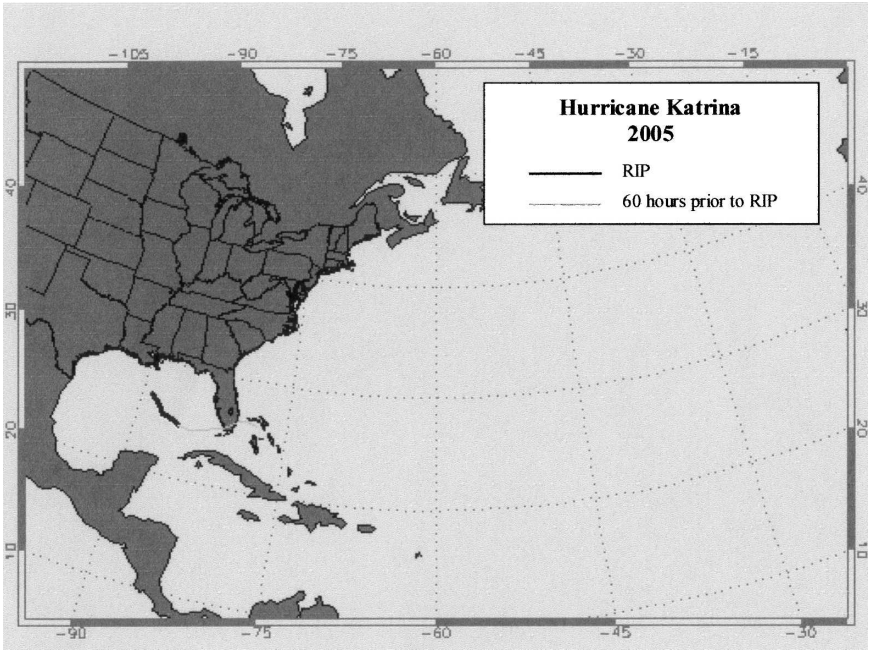

FIG. 6. Track of Hurricane Katrina (2005).

TABLE 10. The model results for Hurricane Katrina. The 24-h WS forecasts are shown with the observed values along with the 24-h pressure forecasts.

Time interval	Model	Model WS increase (kt)	Obs WS increase (kt)	NHC forecast (kt)	CSM (kt)	Model pressure drop (hPa)	Obs pressure drop (hPa)	CSM (hPa)
1*	2	22.68	20	20	12.16	15.05	17	8.75
2*	2	18.98	20	20	12.79	14.36	13	7.81
3*	3	39.57	20	−5	14.98	25.55	16	7.30
4*	3	39.53	20	−25	18.65	27.65	20	6.14
5*	3	40.15	25	−10	21.48	25.49	19	15.46
6*	3	39.96	35	10	17.67	24.65	42	15.40
7*	3	39.74	30	10	14.73	26.25	41	13.70
8*	3	40.26	15	10	12.85	31.64	20	14.14
9	3	40.98	10	25	N/A	32.48	26	N/A
10*	4	10.61	25	15	39.67	7.67	10	34.90
11*	4	13.86	50	15	40.77	7.83	33	35.21
12*	4	13.25	45	15	39.93	11.06	43	35.11
13	4	7.82	40	20	N/A	5.34	35	N/A
14	4	−20.57	5	10	N/A	−6.27	20	N/A
15	4	−33.12	−40	−10	N/A	−19.04	−20	N/A
16	4	−38.61	−80	−85	N/A	−29.36	−58	N/A

* Time intervals that were misclassified by the DFA.

had a central pressure of 965 hPa at time interval 9. However, it did not officially start the RIP until time interval 12 when the central pressure was 945 hPa. This very low pressure leading up to the RIP caused the DFA to predict that it was closer to the RIP than it actually was. Therefore, model 1 was not selected at all, model 2 was selected for time intervals 1 and 2, model 3 was selected for time intervals 3–9, and model 4 was selected to be used from time interval 10 to time interval 16.

The DFA-selected 24-h wind speed model (Table 10) was able to outperform the NHC forecasts on 6 of the 16 time intervals. The intervals where it performed the best were time intervals 3–7 and 15. Even with the misclassifications, model 3 was able to forecast the rapid intensification because of the extraordinarily low MPI [below 850 hPa created by the high SSTs (above 303 K)] throughout the period. This allowed the model to forecast this "secondary" intensification leading up to the RIP and predict the intensification much better than did the NHC model. The NHC forecasted a weakening (time intervals 3–5) as it passed over south Florida; however, both the selected DFA and the CSM suggested otherwise. Because Katrina passed over the Everglades, it did not weaken as it would have if it had passed over drier, more rugged terrain. Model 3 was especially able to capture the rapid intensification, predicting an increase of approximately 40 kt after Katrina reemerged in the Gulf (time intervals 6–7), whereas the NHC only predicted a 10-kt increase. It is interesting to note that during time intervals 8 and 9, the selected model continued to predict a rapid intensification but it did not start until about 18 h later. At these intervals, the heat potential exhibited a significant increase but there was a slight lag response before the extreme rapid intensification took place. For that reason, the CSM (model 2) performed better during time interval 8 because it did not factor the SST as does model 3. From time intervals 10 to 16, the DFA selected model 4 to be used, even though the RIP had not quite started yet. This was because the wind speed was already so high, the central pressure was low, and Katrina had gone through a tremendous amount of intensification that the DFA analyzed that the RIP was in progress. Model 4 did consider the high heat potential; however, this model also considered the high wind speed, longitude, and translational speed, all of which have negative coefficients that predict less intensification. The most intriguing aspect was 6 h before and the onset of the RIP (time intervals 11 and 12), when the selected DFA model and the NHC forecasted similar wind speeds. However, the CSM (model 3) predicted an approximate 40-kt increase, basically forecasting a 140-kt hurricane within 24 h. Katrina eventually achieved wind speeds of 150 kt. Therefore, the CSM only missed the observed value by approximately 10 kt whereas the NHC prediction of 115 kt at the same intervals missed by 35 kt. In summary, the selected DFA models performed well despite the misclassifications until time interval 8, but the CSM would have helped on three more intervals afterward.

The 24-h pressure drop model (Table 10), overall,

had low percentage errors despite the abundance of misclassifications. Usually, model 2 is not an aggressive model, but during time intervals 1 and 2, it forecasted moderate deepening because of the high SSTs (more than 303 K) and the extremely low MPI (approximately 850 hPa). It was more accurate than the CSM (model 1) because it factored these variables. Model 3 was selected to be used from time intervals 3 to 9 and was very aggressive because of the consideration of the core heat potential and the current wind speed. The core heat potential during this period ranged from 40 to 70 kJ cm^{-2} and the wind speed was fairly high (50–90 kt). Even though these intervals were mostly misclassified, these intervals had characteristics of hurricanes that were very close to the RIP. In fact, Katrina went through a "secondary" rapid intensification before undergoing the primary RIP, which likely caused the DFA to select the models it did. Because it was going through the secondary rapid intensification during these time intervals, model 3 was very accurate and more accurate than the CSM. At time interval 9, the DFA-selected model was forecasting a hurricane with an approximate pressure of 933 hPa in 24 h, whereas the observed pressure was 939 hPa. Time intervals 10–12 were also misclassified and model 4 was selected to be used instead of the CSM (model 3). Model 4 greatly underestimated the intensification because of the variables that had negative coefficients, which included MSLP, longitude, and translational speed. The CSM (model 3) would have continued to forecast rapid intensification because of the high core heat potential and wind speed. It was interesting to note that the CSM would have predicted 24-h pressures of approximately 905 and 910 hPa at time intervals 11 and 12, respectively. This proved to be very accurate as Katrina eventually had an extremely low central pressure of 902 hPa at the end of the RIP. Model 4 continued to struggle with time intervals 14 and 16, especially time interval 16, because Katrina was within 24 h of making landfall and these models do not consider inland decay.

d. Average error

The overall performance of the procedures developed to predict RIPs can be evaluated by looking at the average error for each model. Table 11 shows the average error (in hPa) for each 24-h pressure reduction model, both for when the DFA selected the model to be used and for when it should have selected the CSM. When the DFA selected models 1–4, the errors were 4.45, 7.46, 9.70, and 12.06 hPa, respectively. There was a gradual increase in error from model 1 to 4 simply because the magnitude of the error increases as the intensity of the hurricane increases. When model 1 was applied, the hurricane was generally more than 48 h from the RIP and not very intense. However, by the time model 4 was applied, the hurricane was in the RIP and usually intense, making the prediction very difficult. Had these models been correctly selected, the average error would have decreased for all four of these major hurricane models. The CSM for model 3 improved the DFA selection by approximately 4 hPa. Models 5–8 had lower average errors ranging between 1 and 8 hPa. These errors were lower than models 1–4 because models 5–8 were for minor hurricanes and minor hurricanes do not intensify as rapidly or as much, making them easier to forecast. The CSM generally provided improvement except for model 5, where the error slightly increased, and model 8, where the error increased by 1 hPa. This slight increase in error by the CSM was largely due to one point during Hurricane Lisa where the CSM missed the forecast by over 20 hPa. It forecasted a decrease in pressure; however, Lisa was interacting with Hurricane Karl, which caused increased shear that made Lisa weaken. The overall error for the 24-h pressure models was 7.33 hPa as a DFA-selected model and only 5.85 hPa if the CSM would have been used. This shows that the DFA-selected models were accurate considering the error was low and that these particular hurricanes were not easy to forecast because many rapidly intensified. Because the CSM had an even lower error, it shows that this method is very promising and future studies should concentrate on improving the DFA selection process.

TABLE 11. Average error for 24-h pressure drop models in hPa.

	DFA selected	CSM
Model 1	4.45	3.80
Model 2	7.46	5.63
Model 3	9.70	5.80
Model 4	12.06	10.22
Model 5	1.66	1.83
Model 6	6.58	3.11
Model 7	7.81	5.64
Model 8	7.03	8.20
Avg	7.33	5.85

Considering that the official NHC forecast is more accurate on average at the 24-h forecast period than current models used as forecasting guidance by the NHC, it is important to show that the regression models can improve upon their predictions. Table 12 shows the summary of average errors (in kt) for the 24-h wind speed increase models and also shows the average 24-h forecast error by the NHC for the same storms at the same time intervals. When the DFA selected model 1, the average error was 7.95 kt, which was lower than the NHC by almost 2 kt. If model 1 was selected correctly

TABLE 12. Average error for 24-h wind speed increase models in kt.

	DFA selected	CSM	NHC
Model 1	7.95	6.95	9.72
Model 2	11.30	7.83	9.06
Model 3	13.61	7.47	17.36
Model 4	20.06	14.79	13.47
Model 5	2.44	2.93	3.75
Model 6	10.90	4.23	11.00
Model 7	15.11	7.67	15.00
Model 8	16.07	11.96	10.31
Avg	11.83	8.47	12.53

for all time intervals, it would have improved upon the error by an additional 1 kt. Model 2 as the DFA-selected model had a slightly higher error (11.3 kt) than did the NHC (9.06 kt). However, the CSM for model 2 (7.83 kt) would have improved upon the DFA by approximately 3.5 kt, and would have been more accurate than the NHC. The primary reason the DFA-selected model had a higher error was because during Hurricane Ivan, model 2 was used too late in the cycle. Ivan had an unusually high pressure when it started to undergo the RIP and the DFA overestimated the time to the RIP. This caused unusually high errors that affected the average for model 2. When model 3 was selected by the DFA, it improved upon the NHC forecast by approximately 4 kt, but the CSM for model 3 would have improved upon the NHC forecast by approximately 10 kt. Model 3 was able to provide the most improvement over the NHC, as the NHC oftentimes fails to capture the onset of the RIP. However, model 4 (both the DFA selected and the CSM) had higher errors than the NHC. The reason was because of the unusually high errors during Hurricanes Irene and Katrina. Model 4 was misclassified during Irene and produced exceptionally high errors, which explains why there is a large difference between the DFA-selected and the CSM cases (20.06 and 14.79 kt). Also, during Katrina, model 4 was used when landfall was within 24 h. Therefore, it was not able to factor in the inland decay, which even caused the CSM for model 4 to produce high errors. Without these cases, model 4 would have been able to outperform the NHC.

The minor hurricane models (models 5–8) generally outperformed the NHC as well, as both the DFA-selected option and the CSM for models 5 and 6 were more accurate than the NHC. The CSM for model 6 was considerably better, by approximately 7 kt. When the DFA selected model 7, the error was nearly the same as the NHC at comparable time intervals (15.11 and 15 kt). But when the CSM for model 7 was used, the error was only 7.67 kt, improving upon the error by more than 7 kt. As with the major hurricane model (model 3), it was able to forecast particularly well near the onset of the RIP. Model 8 had higher errors than the NHC primarily because it was selected to be used during Alex and Gaston. Toward the end of their RIP, these storms were near the coastline and "skirted" the coastline within 24 h, which caused model 8 to have high error. In summary, the 24-h wind speed models forecasted extremely well compared to the NHC with the exceptions of models 4 and 8 for reasons previously stated. These models had problems because they do not factor for landfall, which therefore caused them to have higher errors. Overall, the DFA-selected models had an average error of 11.83 kt while the NHC had an average error of 12.53 kt. This NHC average error is consistent with other studies, such as Franklin (2005), who observed that the average forecast error for all Atlantic storms was 10.9 kt. However, that study included all storms in the Atlantic and also included the entire track. This caused the average error to be less than the findings here because it included lesser known storms that were not as intense plus it included time periods when the storms were not intensifying rapidly. These weaker storms and other weaker intensification periods have lesser errors because of the magnitude of the intensification. The average 24-h wind speed increase error for the CSM was only 8.47 kt. This was more accurate by 3 kt than the DFA-selected models and more accurate by more than 4 kt than the NHC. The DFA method can be more accurate than the NHC leading up to the RIP and the onset of the RIP, but it can be further improved by getting the DFA to select the correct model. The model needs to be combined with some information about the timing of landfall in order to take into account the dissipative factors associated with landfalls. Other forecast time intervals need to be examined as well to fully improve the aspect of hurricane intensity forecasting.

5. Conclusions

The DFA-selected models for both types (e.g., future 24-h wind speed increase and future 24-h pressure decrease) proved to be beneficial as evidenced by the lower error than the NHC shown in Table 11. Even though the CSM provided substantial improvement, there are a number of improvements that could be made, beginning with the addition of more case studies, which could potentially help expand the DFA selection process. Expanding different forecast periods and the time field beyond the period where the most rapid intensification takes place are also areas for future research. Some hurricanes actually have multiple periods

of rapid intensification, as seen with Hurricane Katrina, which can cause forecasting problems. Inland decay needs to also be addressed, because of the higher errors when a hurricane makes landfall within the 24-h forecast period. The eastern Pacific basin, as well as other basins, needs to be investigated and the models for those basins could then be compared with the Atlantic basin models to see how the intensification factors differ from one basin to another. Instead of averaging the oceanic heat content over a 1° or 5° radius, it could be scaled in terms of the radius of maximum winds to give a more realistic representation.

One caveat, is that this research developed the statistics using reanalysis data instead of real-time observational data, which need to be tested in the future. However, the DFA selection method has been shown to add skill particularly at the 24-h forecast period in terms of both pressure prediction and, especially, wind speed prediction. The NHC consistently struggles with the aspect of rapid intensification and this method shows considerable promise for improving intensification forecasting.

Acknowledgments. The authors thank Joaquin Trinanes and Gustavo Goni for providing us with the tropical cyclone heat potential fields derived at NOAA/AOML.

REFERENCES

Byers, H. R., 1944: *General Meteorology*. McGraw-Hill, 645 pp.

DeMaria, M., and J. Kaplan, 1994: Sea surface temperature and the maximum intensity of Atlantic tropical cyclones. *J. Climate,* **7,** 1324–1334.

——, and ——, 1999: An updated Statistical Hurricane Intensity Prediction Scheme (SHIPS) for the Atlantic and eastern North Pacific basins. *Wea. Forecasting,* **14,** 326–337.

——, M. Mainelli, L. K. Shay, J. A. Knaff, and J. Kaplan, 2005: Further improvements to the Statistical Hurricane Intensity Prediction Scheme (SHIPS). *Wea. Forecasting,* **20,** 531–543.

Franklin, J. L., 2005: 2004 National Hurricane Center forecast verification report. NOAA/NWS/NCEP/Tropical Prediction Center, 26 pp.

Goni, G. J., S. L. Garzoli, A. J. Roubicek, D. B. Olson, and O. B. Brown, 1997: Agulhas ring dynamics from TOPEX/POSEIDON satellite altimeter data. *J. Mar. Res.,* **55,** 861–883.

Gray, W. M., 1968: Global view of the origin of tropical disturbances and storms. *Mon. Wea. Rev.,* **96,** 669–700.

Holland, G. J., 1997: The maximum potential intensity of tropical cyclones. *J. Atmos. Sci.,* **54,** 2519–2541.

Jarvinen, B. R., C. J. Neumann, and M. A. S. Davis, 1984: A tropical cyclone data tape for the North Atlantic basin, 1886–1983: Contents, limitations, and uses. NOAA Tech. Memo. NWS NHC-22, 21 pp. [Available from National Technical Information Service, 5285 Port Royal Rd., Springfield, VA 22161.]

Kalnay, E., and Coauthors, 1996: The NCEP/NCAR 40-Year Reanalysis Project. *Bull. Amer. Meteor. Soc.,* **77,** 437–471.

Kaplan, J., and M. DeMaria, 2003: Large-scale characteristics of rapidly intensifying tropical cyclones in the North Atlantic basin. *Wea. Forecasting,* **18,** 1093–1108.

Knaff, J. A., M. DeMaria, B. Sampson, and J. M. Gross, 2003: Statistical, 5-day tropical cyclone intensity forecasts derived from climatology and persistence. *Wea. Forecasting,* **18,** 80–92.

Law, K., 2001: An investigation of dynamic and thermodynamic effects associated with rapid tropical cyclone intensification. M.S. thesis, Department of Atmospheric Science, The Ohio State University, Columbus, OH, 83 pp.

Lawrence, M. B., L. A. Avila, J. L. Beven, J. L. Franklin, J. L. Guiney, and R. J. Pasch, 2001: Atlantic hurricane season of 1999. *Mon. Wea. Rev.,* **129,** 3057–3084.

Leipper, D., and D. Volgenau, 1972: Hurricane heat potential of the Gulf of Mexico. *J. Phys. Oceanogr.,* **2,** 218–224.

Levitus, S., 1984: Annual cycle of temperature and heat storage in the world's ocean. *J. Phys. Oceanogr.,* **14,** 727–746.

Mainelli, M., 2000: On the role of the upper ocean in tropical cyclone intensity change. M.S. thesis, Dept. of Meteorology and Physical Oceanography, University of Miami, Miami, FL, 73 pp.

Malkus, J. S., and H. Riehl, 1960: On the dynamics and energy transformations in steady-state hurricanes. *Tellus,* **12,** 1–20.

McAdie, C., and M. B. Lawrence, 2000: Improvements in tropical cyclone track forecasting in the Atlantic basin, 1970–98. *Bull. Amer. Meteor. Soc.,* **81,** 989–997.

Merrill, R. T., 1988: Environmental influences on hurricane intensification. *J. Atmos. Sci.,* **45,** 1678–1687.

Miller, B. I., 1958: On the maximum intensity of hurricanes. *J. Meteor.,* **15,** 184–195.

Reynolds, R. W., 1988: A real-time global sea surface temperature analysis. *J. Climate,* **1,** 75–86.

——, and D. C. Marsico, 1993: An improved real-time global sea surface temperature analysis. *J. Climate,* **6,** 114–119.

——, and T. M. Smith, 1994: Improved global sea surface temperature analyses. *J. Climate,* **7,** 929–948.

——, C. L. Gentemann, and F. Wentz, 2004: Impact of TRMM SSTs on a climate-scale SST analysis. *J. Climate,* **17,** 2938–2952.

Saffir, H. S., 1973: Hurricane wind and storm surge. *Military Eng.,* **423,** 4–5.

Shay, L. K., G. J. Goni, and P. G. Black, 2000: Effects of a warm oceanic feature on Hurricane Opal. *Mon. Wea. Rev.,* **128,** 1366–1383.

Simpson, R. H., 1974: The hurricane disaster potential scale. *Weatherwise,* **27,** 169, 186.

Wentz, F. J., and T. Meissner, 1999: AMSR ocean algorithm, version 2. RSS Tech. Rep. 121599A, 66 pp. [Available from Remote Sensing Systems, 438 First St., Ste. 200, Santa Rosa, CA 95401.]

Willoughby, H. E., J. A. Clos, and M. G. Shoreibah, 1982: Concentric eye walls, secondary wind maxima, and the evolution of the hurricane vortex. *J. Atmos. Sci.,* **39,** 395–411.